Erbium Fiber Oscillator With an Intracavity Pulse Shaper for High-Energy Low-Pedestal Wavelength-Tunable Femtosecond Pulse Generation

Hung-Wen Chen, Chia-Lun Tsai, Li-Fan Yang, Ming-Hsien Lin, Kuan-Chen Chu, and Shang-Da Yang, *Member, IEEE*

***Abstract*—An erbium fiber oscillator with dominating gain fiber length and an intracavity pulse shaper is experimentally demonstrated. The Kerr nonlinear phase shift induced in the fibers is suppressed by the pulse shaper, enabling high-energy (8.9 nJ) high-compression efficiency (93%) pulses of less than 270 fs duration (after linear dechirping) at modest (320 mW) pump power. A stably mode-locked spectrum corresponding to 19 nJ, 83 fs transform-limited pulse is achieved at 720 mW pump power. Wave-breaking-free pulse energy can be further enhanced by introducing stronger spectral phase modulation via the pulse shaper if more pump budget is available. We also demonstrate manipulation of the central wavelength and bandwidth of the output pulse by intracavity spectral amplitude modulation via the pulse shaper.**

***Index Terms*—Dissipative soliton, erbium-doped fiber amplifier (EDFA), mode-locked fiber lasers, pulse shaper, similariton.**

I. Introduction

HIGH-energy (>1 nJ) mode-locked fiber oscillators receive increasing attention because of their compactness, low cost, and versatile applications such as nonlinear microscopy [1], [2] and frequency comb spectroscopy [3]. However, pulse energies of conventional soliton and stretched-pulse [4] fiber lasers are limited by ~0.1 nJ and ~1 nJ, respectively [5]. For example, a stretched-pulse erbium-doped fiber (EDF) laser was demonstrated to produce 31.8 MHz, 105 fs, 2.7 nJ pulse [6]. Self-similar evolution in normally dispersive fibers has been employed by passive-similariton, dissipative-soliton, amplifier-similariton lasers to deliver pulses of higher energies, where the round-trip self-consistency is achieved by anomalously dispersive delay line or spectral filter, respectively [5], [7].

Several factors restrict the maximum pulse energy of these fiber oscillators. 1) Multi-pulsing could arise from overdriving the saturable absorber [8], [9]. 2) Pulse will break up (wave-breaking) in the presence of excessive Kerr nonlinear phase shift [10]. 3) Self-similar evolution in a gain fiber will be disrupted when the broadened spectrum approaches the limit of gain bandwidth. The resulting spectral distortion and nonlinear chirp may deteriorate the pulse compression efficiency (defined as the ratio between the energy in the clean center and the total energy of a linearly dechirped pulse) [11]. In addition to using large-mode-area gain fiber to reduce the intensity and nonlinearity [12], dissipative-soliton lasers typically overcome these problems by employing long passive fiber and short gain fiber to linearize the pulse chirp and suppress the spectral broadening induced in the gain fiber [13]. Nevertheless, transplanting this strategy from ytterbium to erbium fiber oscillators is challenging because 1) the standard single-mode fiber (SMF) exhibits anomalous dispersion in the lasing wavelengths (~1550 nm), while the EDF core has to be small (subject to strong nonlinearity) to achieve normal dispersion, 2) longer EDF is normally needed to provide high gain due to the lower doping concentration, 3) EDF has narrower gain bandwidth. An erbium fiber oscillator delivering 3.5 MHz, 750 fs (linearly dechirped), 20 nJ pulses with strong oscillatory tail (56% compression efficiency) was demonstrated by using long (58 m) passive fiber, short (59 cm) EDF, and 1.2 W pump power [14].

In this paper, we report on a high-energy, low-pedestal, and wavelength-tunable erbium fiber oscillator with dominating (normally dispersive) EDF length and an intracavity pulse shaper. The long EDF permits the amplifier-similariton operation [7], while the problems of multi-pulsing, wave-breaking, and finite gain bandwidth are alleviated by adding a large amount of normal group delay dispersion (GDD) via the pulse shaper without incurring extra nonlinearity (in contrast to simultaneously adding GDD and nonlinearity by bulk material or long dispersion compensating fiber in [12], and [15]). In this way, 8.3 MHz, 268 fs (linearly dechirped), 8.9 nJ stable pulse train (with 67% compression efficiency) was produced at a much lower pump power of 320 mW. We also substantially suppressed the temporal intensity pedestal or oscillatory tail (suffered by high-energy mode-locked fiber oscillators [12], [14]) by introducing adequate cubic spectral phase modulation via the intracavity pulse shaper, leading to 184 fs pulse (linearly dechirped) with 93% compression efficiency. A stably mode-locked spectrum corresponding to 19 nJ, 83 fs transform-limited (TL) pulse

Manuscript received December 6, 2013; revised June 20, 2014 and February 7, 2014; accepted June 23, 2014. Date of publication June 26, 2014; date of current version August 15, 2014. This work was supported in part by the National Science Council in Taiwan under Grant NSC 100-2221-E-007-093-MY3, and the National Tsing Hua University under Grant 102N2081E1.

The authors are with the Institute of Photonics Technologies, National Tsing Hua University, Hsinchu 30013, Taiwan (e-mail: h.w.chen0427@gmail.com; tsaichalun@gmail.com; lifan.yang1986@gmail.com; bravo.physics@gmail.com; allenzhen80@gmail.com; shangda@ee.nthu.edu.tw).

Color versions of one or more of the figures in this paper are available online at http://ieeexplore.ieee.org.

Digital Object Identifier 10.1109/JLT.2014.2333654

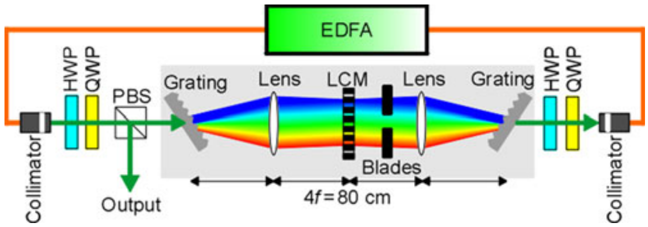

Fig. 1. Experimental setup. QWP: quarter wave plate; HWP: half wave plate; PBS: polarization beam splitter; LCM: liquid crystal modulator.

was achieved at 720 mW pump power. Wide-range tuning of the central wavelength (1537–1566 nm) and bandwidth (20–29 nm) of the output pulse was achieved by performing intracavity spectral amplitude modulation. Although tunable intracavity spectral amplitude [16] or phase [17] modulation has been implemented in semiconductor or solid-state lasers, the intracavity shaping in fiber lasers has a more profound impact on pulse formation due to the stronger light-matter interaction.

II. Setup and Performances in the Absence of Intracavity Spectral Phase Shaping

The experimental setup is shown in Fig. 1. A customized erbium-doped fiber amplifier (EDFA, GIP Tech) contains 17-m-long EDF ($\beta_2 = 22.2\,\mathrm{ps}^2/\mathrm{km}, \beta_3 = 0.23\,\mathrm{ps}^3/\mathrm{km}$) and 4.7-m-long lead SMF ($\beta_2 = -21.9\,\mathrm{ps}^2/\mathrm{km}, \beta_3 = 0.60\,\mathrm{ps}^3/\mathrm{km}$), contributing to a net cavity GDD of 0.27 ps^2 at 1560 nm wavelength. A liquid crystal spatial light modulator (SLM-128-D-NM, CRI) and two blades are placed on and after the focal plane of a homemade 4-f pulse shaper to modulate the spectral phase and amplitude, respectively. The spectral window and resolution of the pulse shaper are 1524–1576 nm and 0.4 nm, capable of introducing an extra GDD up to 63.6 ps^2. Mode-locking is initiated and stabilized by nonlinear polarization evolution (NPE) through adjusting two pairs of half- and quarter-wave plates. Intensity autocorrelation (IA) or frequency-resolved optical gating (FROG) is used to measure the temporal waveform of the output pulse. The pulse-to-pulse stability is characterized by oscilloscope trace, long-range IA trace, and radio frequency (RF) spectral analysis [18].

By operating the oscillator at 1550 nm filter central wavelength, 5.3 nm filter bandwidth, 320 mW pump power, and zero spectral phase modulation, we could get a stably mode-locked pulse train of 8.3 MHz repetition rate and 8.9 nJ energy. Characterization results of this pulse train are illustrated in Fig. 2. The output power spectrum [see Fig. 2(a)] spanning over 1520–1588 nm corresponds to a TL pulse width (FWHM) of 146 fs (364 fs in [14]). The pump threshold for the continuous-wave (CW) mode and the slope rate efficiency of the CW and mode-locking modes are 47 mW and ∼33%, respectively [see Fig. 2(b)]. Fig. 2(c) shows the IA traces before (dashed) and after (solid) linear dechirping by a grating compressor, where the correlation widths (FHWM) are 2.4 ps and 387 fs, respectively. The small residual chirp (before dechirping) together with the

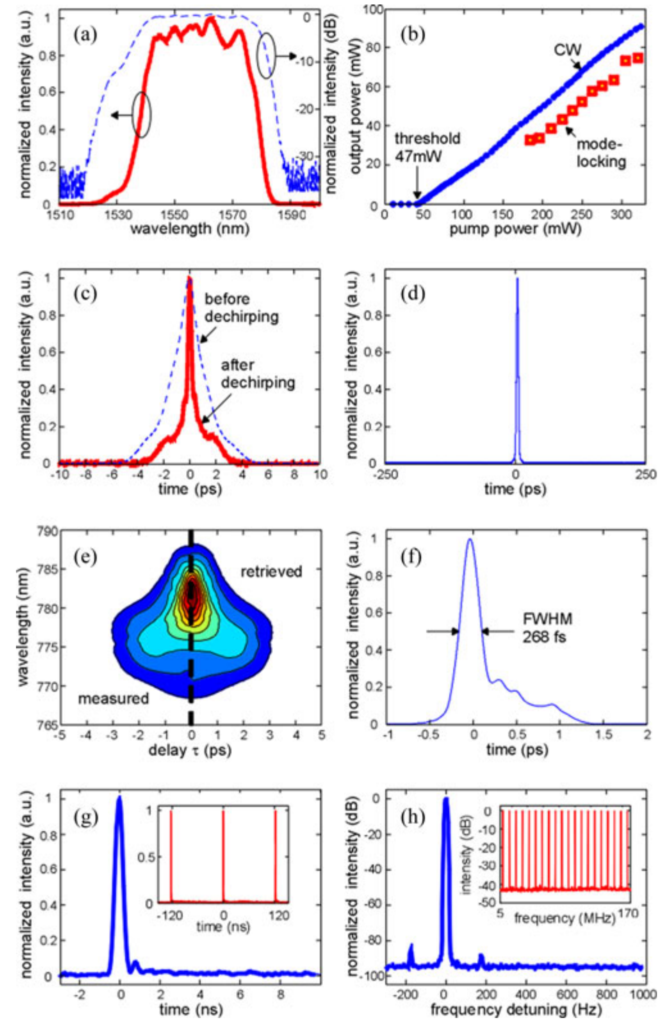

Fig. 2. Characterization results for the oscillator operated at 1550 nm filter center, 5.3 nm filter bandwidth, 320 mW pump power, and no spectral phase modulation from the shaper. (a) Power spectrum in linear (solid) and log (dashed) scales. (b) The output power versus pump power when the laser operates at CW mode (circles) and mode-locking mode (squares). (c) The intensity autocorrelation traces before (dashed) and after (solid) linear dechirping by a grating compressor. (d) Long range intensity autocorrelation trace. (e) Measured (left) and retrieved (right) FROG traces. (f) Temporal intensity of the linearly dechirped pulse retrieved by FROG. (g) Oscilloscope traces. (h) RF spectra centered at 8.3 MHz with 1 Hz resolution, and from 5 to 170 MHz with 20 Hz resolution (inset).

lack of steep spectral edges suggests the amplifier-similariton operation of the oscillator [7]. Note that, the IA functions are distinct from the coherence spike with 2:1 or 2:1:0 contrast ratio due to CW noise or finite-duration noise burst, respectively [19]. Fig. 2(d) illustrates the IA trace scanned over 500 ps, indicating that there is no extra pulse within the 250 ps time window.

Fig. 2(e) shows the measured (left) and retrieved (right) FROG traces of the linearly dechirped pulse. The pedestal-free FROG traces and the low (0.005) FROG error strongly suggest stable mode-locking operation [20]. The retrieved temporal intensity [see Fig. 2(f)] has 268 fs duration (FWHM), corresponding to a reasonable deconvolution factor (1.44) for the IA trace. The pedestal on the trailing edge (containing 33% of the pulse

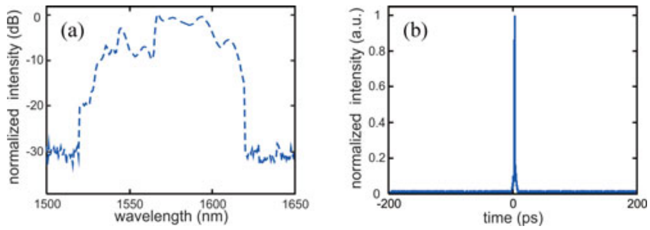

Fig. 3. (a) Power spectrum, and (b) long range intensity autocorrelation trace obtained at 720 mW pump power.

energy) extends over 1 ps range, consistent with the IA pedestal width. The achieved peak power is 6.2 kW (considering the 30% grating compressor efficiency), higher than that (~4.9 kW) achieved in [14]. The pulse train dynamics is characterized by a 4 GHz oscilloscope (DSO80404B, Agilent), a 50 GHz photo detector (XPDV2120R-VF-FP, μ2t), and a 44 GHz electrical spectrum analyzer (N9030A PXA-544, Agilent). The oscilloscope traces [see Fig. 2(g)] exhibit stable periodic pulses, verifying the single-pulse (during the ~1–120 ns window) and CW mode-locking operation of the oscillator. The RF spectrum [see Fig. 2(h)] shows narrow linewidth, equally spaced peaks, uniform peak amplitudes, and high (–43 dB) side mode suppression [see inset of Fig. 2(h)]. The amplitude noise and timing jitter calculated by RF spectral analysis [19] are 0.23% and 2.25 ps (18 ppm), respectively. These results would not be possible for broadband noise or a train of noise bursts, further confirming that our oscillator did produce a stable train of isolated pulses.

Fig. 3 shows that our oscillator is potentially able to produce sub-100 fs pulses. By increasing the pump power to 720 mW and increasing the EDF length to 30 m, a broader power spectrum spanning over 1520–1620 nm was obtained [see Fig. 3(a)]. The single-pulse and CW mode-locking operation was experimentally verified by long-range IA trace [see Fig. 3(b)] and oscilloscope trace (not shown here). The pulse energy increased to 19 nJ, while the corresponding TL pulse width (83 fs) became comparable to that (77 fs) achieved by stretched-pulse ring lasers [4]. Even shorter pulses could arise by inserting a highly nonlinear fiber (HNLF) inside the cavity, where a pulse shorter than the gain-bandwidth limitation (21 fs) has been generated from a self-similar fiber laser [21].

To demonstrate the high peak power of our fiber oscillator, we roughly dechirped the output pulse by a 8-m-long SMF and coupled 2 nJ pulse into a 30-m-long dispersion-shifted HNLF $(\gamma = 10\,\mathrm{W}^{-1}/\mathrm{km}, \beta_2 = 0.28\,\mathrm{ps}^2/\mathrm{km})$ for spectral broadening. As shown in Fig. 4, the output power spectrum measured by an optical spectrum analyzer (AQ6375, Yokogawa) extends beyond 1200–2000 nm. The broad bandwidth can support a TL pulse of 13 fs duration. The rapid roll-off of the two spectral wings is mainly attributed to the strong OH^- impurity absorption and infrared absorption of the silica fiber, where the latter can be alleviated by using chalcogenide or tellurite HNLF. The supercontinuum source could provide femtosecond pulse centered around 1700 nm, which is useful in deep tissue *in vivo* multiphoton microscopy [2].

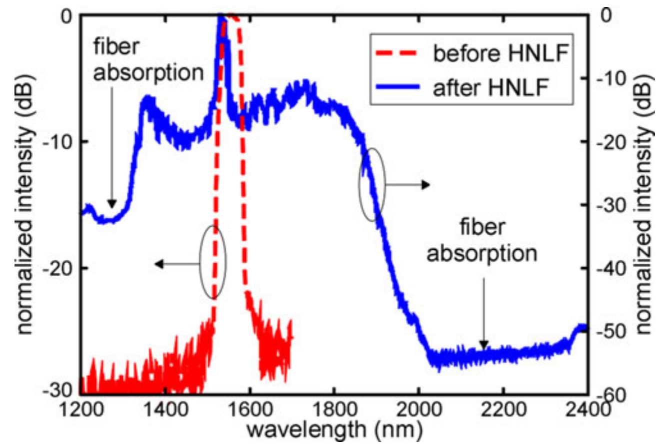

Fig. 4. The power spectra before (dashed) and after (solid) passing through a 15-m-long HNLF, respectively.

III. Impacts of Intracavity Pulse Shaper

Fig. 5 illustrates that extra GDD added by the intracavity pulse shaper can suppress wave-breaking at higher pump powers. Fig. 5(a) displays the power spectra (individually normalized to unit peak for clarity) measured at different pump powers when a narrower filter bandwidth of 4.3 nm is used (closer to wave-breaking [5]). In the absence of extra GDD (left of the vertical dashed line), the pulse train remains stable until the amplitude noise and timing jitter suddenly rise at a pump power of 204 mW [see Fig. 5(c)]. Further increasing the pump power will cause wave-breaking. The pulse energy of a stable train (at 4.3 nm filter bandwidth) is limited by 3.9 nJ, occurring at a critical pump power of 196 mW. By adding an extra GDD (D_{g+}) of 0.18 ps^2 via the pulse shaper at the same pump power, the rms bandwidth drops from 21 to 15 nm while the output pulse energy is roughly maintained [see Fig. 5(b)]. The inset across Fig 5(b) and (c) illustrates the IA traces of the linearly dechirped pulses before (solid) and after (dashed) adding the 0.18 ps^2 extra GDD at 196 mW pump power, respectively. The reduced bandwidth and weaker IA pedestal imply that extra GDD can suppress the Kerr nonlinear phase shift accumulated in the fibers and drive the oscillator away from wave-breaking. As a result, we could crank up the pump power to 320 mW without disrupting the mode-locking (right of the vertical dashed line in Fig. 5). The corresponding pulse energy is 8.9 nJ, limited by our pump budget.

Since the pulse shaper permits arbitrary spectral modulation, an extra cubic phase can be introduced to improve the pulse compression efficiency by partially compensating the intracavity nonlinear chirp due to Kerr nonlinear phase shift or the higher order dispersion of the fibers. Fig. 6 shows the pulse compression efficiency versus the added cubic spectral phase coefficient Ψ_{3+} at the maximum pump power of 320 mW, where three (out of seven) temporal intensities of the linearly dechirped pulses (retrieved by FROG and numerical quadratic spectral phase compensation) are illustrated for comparison (insets). The peak compression efficiency (93%) occurs at $\Psi_{3+} = -8.1 \times 10^{-4}$ ps^3, while a high compression efficiency

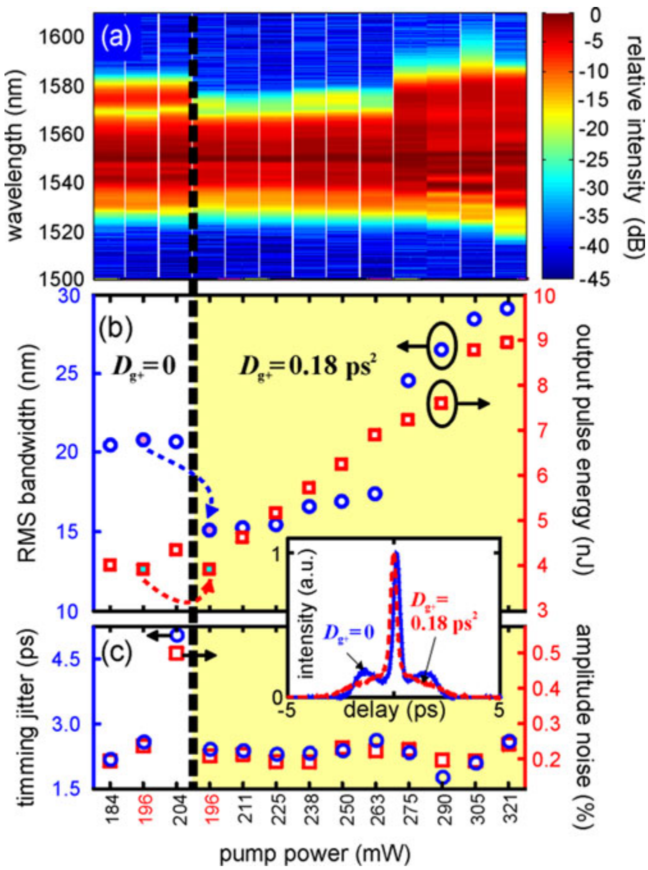

Fig. 5. (a) Power spectrum, (b) rms bandwidth (circles), pulse energy (squares), (c) timing jitter (circles), amplitude noise (squares) of the output pulse as a function of pump power before (left of the dashed line) and after adding an extra GDD ($D_{g,+}$) of 0.18 ps^2 via the intracavity pulse shaper. The filter pass-band is centered at 1550 nm and spans 4.3 nm. Inset: The IA functions of the linearly dechirped output pulses at 196 mW pump power before (solid) and after (dashed) applying the extra GDD.

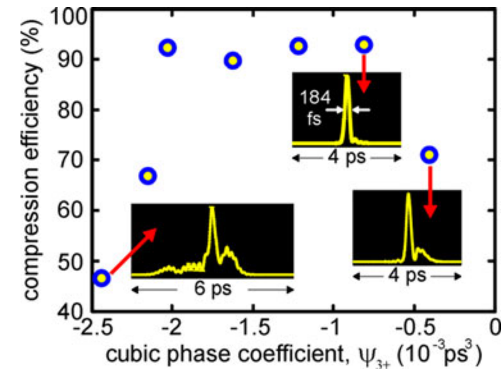

Fig. 6. Pulse compression efficiency versus the intra-cavity cubic phase coefficient. The filter pass-band is centered at 1550 nm and spans 5.6 nm. Inset: Time domain pulses retrieved by frequency-resolved optical gating (FROG) measurement and numerical linear dechirping.

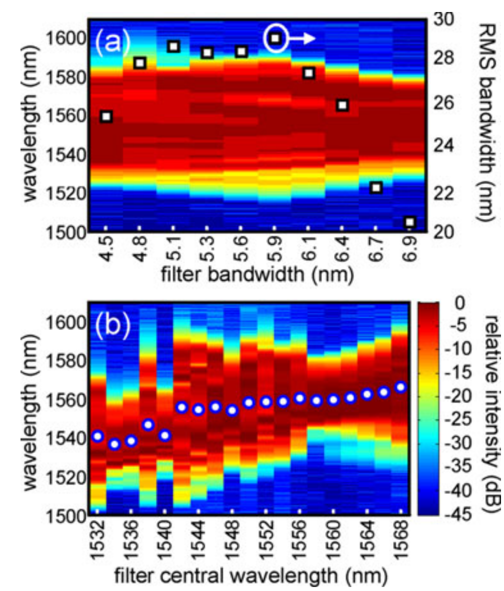

Fig. 7. The output spectra versus (a) the filter bandwidth (centered at 1550 nm), and (b) the filter central wavelength (with 5.3 nm bandwidth), respectively. All are operated at 321-mW pump power and zero extra phase modulation.

plateau (~90%) exists when Ψ_{3+} is between -8×10^{-4} ps^3 and -2×10^{-3} ps^3. Cubic spectral phase modulation outside the plateau region will rapidly degrade the compression efficiency and even destabilize the mode locking. Since the cubic phase coefficient due to the EDF and SMF (-6.7×10^{-3} ps^3) is larger in magnitude and of the same sign, the added Ψ_{3+} is expected to compensate the Kerr nonlinear phase shift. Compared with the pulses linearly dechirped outside the cavity shown in Fig. 2(f) of this paper and the inset of Fig. 3(d) in [14], it is evident that adequate cubic phase modulation introduced by an intracavity pulse shaper can substantially improve the quality and peak power (~13 kW in this case, after taking the 30% grating compressor efficiency into account) of the output pulse. Although the pedestal level (<6%, defined as the highest sidelobe peak relative to the main peak) remains much higher than that (~10^{-5}) of a stretched-pulse laser demonstrated in [22], the latter was achieved under 29 pJ energy (300 times weaker than our case). Note that, simpler configurations or devices (e.g., four prisms) can be used to achieve spectral modulation of limited degree of freedom. The requirement of adequate cubic phase modulation justifies the employment of an intracavity pulse shaper in this study.

Fig. 7(a) and (b) shows the power spectra measured at 320 mW pump power and different spectral amplitude modulation conditions. In view of the nontrivial spectral shapes, the central wavelength and bandwidth are evaluated by the weighted average values [18]. At a fixed filter center of 1550 nm, the rms bandwidth of the output pulse is maximized at a filter bandwidth of ~5.9 nm. Mode-locking becomes unstable if the filter bandwidth is outside the range of 4.5–6.9 nm [see Fig. 7(a)], primarily because of the interplay among the effects of self-amplitude modulation, cavity loss, and gain bandwidth [23]. At a fixed filter bandwidth of 5.3 nm, the output spectral center [circles, Fig. 7(b)] could be tuned from 1537 to 1566 nm as the filer central wavelength varies from 1532 to 1568 nm. These results demonstrate the great flexibility of the oscillator enabled by the intracavity spectral amplitude modulation.

IV. Conclusion

In summary, an erbium fiber oscillator with long EDF and an intracavity pulse shaper was established, producing wavelength-tunable femtosecond pulses with 8.9 nJ energy at 320 mW pump power. The single-pulse and CW mode-locking operation of the oscillator was systematically verified by IA, FROG, RF spectral analysis, and supercontinuum generation experiments. By increasing the pump power and EDF length to 720 mW and 30 m, a stably mode-locked spectrum corresponding to 83 fs TL pulse width and 19 nJ pulse energy was obtained. The use of long EDF (instead of long passive fiber) greatly facilitates the construction of high-energy erbium fiber oscillators, and the extra GDD introduced by the pulse shaper effectively solves the energy-limiting problems inherited by using long gain fibers. The pedestal or oscillatory tail of high-energy output pulse can be substantially suppressed by intracavity cubic phase modulation via the pulse shaper, leading to 93% pulse compression efficiency at 8.9 nJ. The marriage of fiber oscillator and pulse shaper provides a platform to experimentally explore the rich phenomena of dissipative solitons [23].

Acknowledgment

The authors would like to thank GIP Technology Corporation, Dr. C. B. Huang of NTHU, and Dr. Y. S. Ku and Dr. J. L. Peng of Industrial Technology Research Institute of Taiwan for customizing the EDFA and technical supports, respectively.

References

[1] F. W. Wise, "Femtosecond fiber lasers based on dissipative processes for nonlinear microscopy," *IEEE J. Quantum Electron.*, vol. 18, no. 4, pp. 1412–1421, Jul. 2012.

[2] N. G. Horton, K. Wang, D. Kobat, C. G. Clark, F. W. Wise, C. B. Schaffer, and C. Xu, "In vivo three-photon microscopy of subcortical structures within an intact mouse brain," *Nature Photon.*, vol. 7, pp. 205–209, Mar. 2013.

[3] T. R. Schibli, I. Hartl, D. C. Yost, M. J. Martin, A. Marcinkevicius, M. E. Fermann, and J. Ye, "Optical frequency comb with submillihertz linewidth and more than 10 W average power," *Nature Photon.*, vol. 2, pp. 355–359, Jun. 2008.

[4] K. Tamura, E. P. Ippen, H. A. Haus, and L. E. Nelson, "77-fs pulse generation from a stretched-pulse mode-locked all-fiber ring laser," *Opt. Lett.*, vol. 18, no. 13, pp. 1080–1082, Jul. 1993.

[5] F. W. Wise, A. Chong, and W. H. Renninger, "High-energy femtosecond fiber lasers based on pulse propagation at normal dispersion," *Laser Photon. Rev.*, vol. 2, no. 1–2, pp. 58–73, Feb. 2008.

[6] L. E. Nelson, S. B. Fleischer, G. Lenz, and E. P. Ippen, "Efficient frequency doubling of a femtosecond fiber laser," *Opt. Lett.*, vol. 21, no. 21, pp. 1759–1761, Jul. 1996.

[7] W. H. Renninger, A. Chong, and F. W. Wise, "Self-similar pulse evolution in an all-normal-dispersion laser," *Phys. Rev. A*, vol. 82, no. 2, p. 021805, Aug. 2010.

[8] A. Komarov, H. Leblond, and F. Sanchez, "Multistability and hysteresis phenomena in passively modelocked fiber lasers," *Phys. Rev. A*, vol. 71, no. 5, p. 053809, May 2005.

[9] J. Buckley, A. Chong, S. Zhou, W. H. Renninger, and F. W. Wise, "Stabilization of high-energy femtosecond ytterbium fiber lasers by use of a frequency filter," *J. Opt. Soc. Amer. B*, vol. 24, no. 8, pp. 1803–1806, Aug. 2007.

[10] W. J. Thomlinson, R. H. Stolen, and A. M. Johnson, "Optical wave breaking of pulses in nonlinear optical fibers," *Opt. Lett.*, vol. 10, no. 9, pp. 457–459, Sep. 1985.

[11] D. B. S. Soh, J. Nilsson, and A. B. Grudinin, "Efficient femtosecond pulse generation using a parabolic amplifier combined with a pulse compressor. II. Finite gain-bandwidth effect," *J. Opt. Soc. Amer. B*, vol. 23, no. 1, pp. 10–19, Jan. 2006.

[12] M. Baumgartl, F. Jansen, F. Stutzki, C. Jauregui, B. Ortaç, J. Limpert, and A. Tünnermann, "High average and peak power femtosecond large-pitch photonic-crystal-fiber laser," *Opt. Lett.*, vol. 36, no. 2, pp. 244–246, Jan. 2011.

[13] A. Chong, W. H. Renninger, and F. W. Wise, "All-normal-dispersion femtosecond fiber laser with pulse energy above 20 nJ," *Opt. Lett.*, vol. 32, no. 16, pp. 2408–2410, Aug. 2007.

[14] N. B. Chichkov, K. Hausmann, D. Wandt, U. Morgner, J. Neumann, and D. Kracht, "High-power dissipative solitons from an all-normal dispersion erbium fiber oscillator," *Opt. Lett.*, vol. 35, no. 16, pp. 2807–2809, Aug. 2010.

[15] C. M. Ouyang, P. P. Shum, K. Wu, J. H. Wong, X. Wu, H. Q. Lam, and S. Aditya, "Dissipative soliton (12 nJ) from an all-fiber passively mode-locked laser with large normal dispersion," *IEEE Photon. J.*, vol. 3, no. 5, pp. 881–887, Oct. 2011.

[16] S. Gee, G. A. Alphonse, J. C. Connolly, C. Barty, and P. J. Delfyett, "Ultrashort pulse generation by intracavity spectral shaping and phase compensation of external-cavity modelocked semiconductor lasers," *IEEE J. Quantum Electron.*, vol. 36, no. 9, pp. 1035–1040, Sep. 2000.

[17] N. K. Metzger, W. Lubeigt, D. Burns, M. Griffith, L. Laycock, A. A. Lagatsky, C. T. A. Brown, and W. Sibbett, "Ultrashort-pulse laser with an intracavity phase shaping element," *Opt. Exp.*, vol. 18, no. 8, pp. 8123–8134, Apr. 2010.

[18] A. M. Weiner, "Characterization of noise and jitter," in *Ultrafast Optics*, 1st ed. Hoboken, NJ, USA: Wiley, 2009, pp. 139–144.

[19] A. M. Weiner, "Intensity correlation measurements," in *Ultrafast Optics*, 1st ed. Hoboken, NJ, USA: Wiley, 2009, pp. 99–112.

[20] M. Rhodes, G. Steinmeyer, J. Ratner, and R. Trebino, "Pulse-shape instabilities and their measurement," *Laser Photon. Rev.*, vol. 7, no. 4, pp. 557–565, Jul. 2013.

[21] P. Grelu and N. Akhmediev, "Dissipative solitons for mode-locked lasers," *Nature Photon.*, vol. 6, pp. 84–92, Feb. 2012.

[22] H. A. Haus, K. Tamura, L. E. Nelson, and E. P. Ippen, "Stretched-pulse additive pulse mode-locking in fiber ring lasers: Theory and experiment," *IEEE J. Quantum Electron.*, vol. 31, no. 3, pp. 591–598, Mar. 1995.

[23] A. Chong, H. Liu, B. Nie, B. G. Bale, S. Wabnitz, W. H. Renninger, M. Dantus, and F. W. Wise, "Pulse generation without gain-bandwidth limitation in a laser with self-similar evolution," *Opt. Exp.*, vol. 20, no. 13, pp. 14213–14220, Apr. 2012.

Hung-Wen Chen received the B.S. degree from the College of Technology Management in 2011, and the M.S. degree from the Institute of Photonics Technologies in 2013, both from National Tsing Hua University, Hsinchu, Taiwan. His research interests include femtosecond fiber oscillators.

Chia-Lun Tsai received the B.S. degree in electrical engineering in 2010, and the M.S. degree from the Institute of Photonics Technologies in 2013, both from National Tsing Hua University, Hsinchu, Taiwan, where he is currently working toward the Ph.D. degree with the Institute of Photonics Technologies. His research interests include femtosecond fiber oscillators, high-power optical parametric amplifiers, and femtosecond pulse measurement.

Li-Fan Yang received the B.S. degree in electrical engineering in 2009 and the M.S. degree from the Institute of Photonics Technologies in 2012, both from National Tsing Hua University, Hsinchu, Taiwan. He is currently working toward the Ph.D. degree with Purdue University, West Lafayette, IN, USA. His research interests include fiber oscillators and nonlinear optics.

Ming-Hsien Lin received the B.S. degree in physics from National Tsing Hua University, Hsinchu, Taiwan, in 2012, where he is currently working toward the M.S. degree with the Institute of Photonics Technologies. His research interests include noise properties of mode-locked lasers and comb characterization.

Kuan-Chen Chu received the B.S. degree in electrical engineering from National Tsing Hua University, Hsinchu, Taiwan, in 2013, where he is currently working toward the M.S. degree with the Institute of Photonics Technologies. His research interests focus on femtosecond fiber oscillators.

Shang-Da Yang (S'01–M'05) was born in Chiayi, Taiwan, in 1975. He received the B.S. degree in electrical engineering from National Tsing Hua University, Hsinchu, Taiwan, in 1997, the M.S. degree in electro-optical engineering from National Taiwan University, Taipei, Taiwan, in 1999, and Ph.D. degree from the School of Electrical and Computer Engineering, Purdue University, West Lafayette, IN, USA, in 2005, respectively. He joined National Tsing Hua University, Hsinchu, Taiwan, in 2005 as Assistant Professor, and was promoted to an Associate Professor in 2010. He received the RiTEK Young Investigator Medal of the Optical Engineering Society of the Republic of China in 2007. He was a visiting Professor in Joint Institute for Laboratory Astrophysics, University of Colorado at Boulder, Boulder, CO, USA, in 2011. His research interests include ultrasensitive femtosecond pulse measurements, characterizations of optical frequency combs, quasi-phase matching engineering, and femtosecond fiber oscillators.